JOURNAL OF MATERIALS SCIENCE 19 (1984) 3498–3514

The fatigue properties of dynamically consolidated aluminium

D. RAYBOULD
Materials Laboratory, Corporate Technology, Allied Corporation, Morristown, New Jersey 07960, USA

Dynamic consolidation produces material made up of work-hardened particles bonded together by ultra rapidly solidified welds. Obviously such a structure will have unique mechanical properties. It has been found that the fatigue strength at 10^7 cycles of dynamically consolidated aluminium is significantly above that of wrought ingot metallurgy material of similar composition. Annealing the compacts at 300° C only slightly reduces the fatigue strength. However, there is an appreciable reduction after annealing at 400° C and above. The fatigue strength appears equal to one-half the yield strength; a more complex relationship exists for the ultimate strength. The fatigue strength, like the yield strength, is probably related to the ratio R, which predicts the degree of interparticle melting. The value of this ratio may be calculated. The compacts undergo an insignificant amount of cyclic softening during low-cycle fatigue tests, although some softening does occur in specimens annealed at 300° C. Microscopy indicates that failure is of a ductile interparticular nature with some evidence of small areas of fatigue striations and "ridges". The results, especially the reduction in properties on annealing, suggest that the improved fatigue properties reported for aluminium are a direct result of dynamic consolidation. Application to other alloys is, therefore, logical. The degree will depend upon the amount of work-hardening and of ultra rapidly solidified welding the alloy experiences.

1. Introduction

The limiting property for many material applications is the fatigue strength. A substantial interest in improving fatigue properties and maintaining them during production is therefore natural. Powder metallurgy (PM) is one technique which has been employed for aluminium [1–3], steels [4] and superalloys [5, 6]. The ability to consolidate powders to full density has allowed the exploitation of the finer metallurgical structures of powders that result from their higher solidification rates. PM also avoids, or reduces in magnitude, anisotropy, macro-segregation and impurities. For the latter, good housekeeping allows the size of contaminants compacted with the powder to be reduced, thus allowing further improvements [7]. However, wrought PM techniques which produce material flow, such as extrusion or powder forging, are probably less susceptible to contaminants than hot isostatic pressing type techniques. Flow after, or during, the final stages of consolidation improves fatigue resistance because of the breakdown of surface oxide films [2, 8] and, probably, the development of substructure. For example, ingot metallurgy (IM) aluminium alloys containing sub-grains have, as would be expected, superior fatigue properties to similar alloys without sub-grains [9]. However, once the substructure is formed, parameters such as the temperature-compensated strain rate (Z) may surprisingly not be extremely important [10], despite the importance of this parameter in respect to the final substructure [11].

It is well known that work-hardening, especially of the surface layers, increases fatigue resistance, in particular at low strain (stress) conditions. One reason for this is probably that the initially higher dislocation density results in more homogeneous slip and thus less damage [12].

0022–2461/84 $03.00 + .12

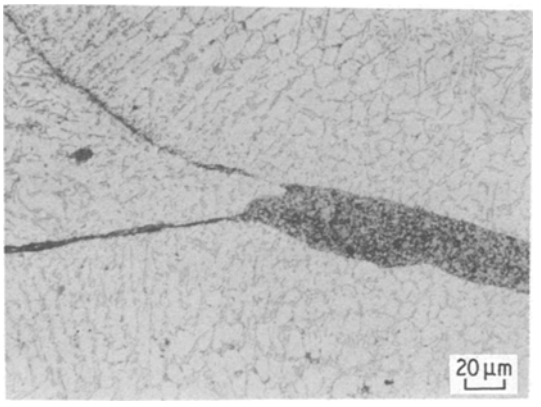

Figure 1 Melting and bonding between three particles of water-atomized Al–12%Si, Note the refinement of structure.

Dynamic powder compaction (DPC) allows the compaction and interparticle bonding of powders at room temperature [13, 14], so allowing the fine structure of the powder to be fully retained if required; this is not possible with the normal hot consolidation or sintering operations. Similarly, the work- or shock-hardening that occurs during dynamic compaction is retained, and not annealed out by sintering. This work- or shock-hardening can produce hardness values appreciably above those attained by conventional mechanical working operations and even above that attained with explosive hardening [14, 15]. It is believed that to allow deformation in such short times, a large number of dislocations moving short distances must be involved; these dislocations are probably similar to those proposed for explosive hardening [16]. In addition, DPC produces extensive material flow and/or a rapidly solidified weld zone at the particle's interface [13–15], so breaking up the oxide film around the particles. The effect of the rapidly solidified weld zone (Fig. 1) is difficult to estimate in view of the sparsity of data on the fatigue strength of material solidified at cooling rates of over 10^6 °C sec^{-1}. A fine microcrystalline structure should be advantageous and thin strips of amorphous Metglas®* have good fatigue properties, at high stresses [17] although high cycle life is disappointing. Moreover, the importance of this melted zone is demonstrated by the original oxide dispersion hardened aluminium, SAP, the poor fatigue strength of which, despite the apparently desirable structure, was attributed to the weak alumina–aluminium interfaces [12].

The potential benefits of the highly work-hardened particles, the retention of the powders original fine structure, the interparticle shearing and the rapidly solidified weld zone, make the determination of the fatigue properties of dynamically consolidated material very interesting. At present, the only work on the fatigue properties of dynamic compacts has been carried out in the USSR on material produced by hot explosive compaction. However, the high temperatures involved would be expected to destroy many of the advantages that could be anticipated with material produced by DPC. Properties equivalent to those of the wrought material were, however, reported [18].

To determine the fatigue properties of material consolidated dynamically, it was decided to investigate the properties of a material known to undergo appreciable work-hardening, and because of the interest in and the information that was readily available, aluminium was chosen as the test material. Existing ingot metallurgy alloys are well documented and several works on PM alloys have already been mentioned [1–3, 8, 10] and a review [19] has considered the properties of various PM alloys.

An additional reason for the choice of aluminium was the low fatigue-to-tensile strength ratio of high-strength aluminium alloys. For instance, while ratios of 0.4 to 0.5 are usual with most metals, the high tensile strength, fully treated IM 7075-T6 alloy has a ratio of 0.28. The lower strength, non-treated IM 5086-0 alloy actually has a similar fatigue strength due to its higher ratio, 0.5 [20]. Therefore, more so than with other materials, fatigue is a limiting property for high-strength aluminium.

The special advanced aluminium alloys and powders were thought to offer too many complications for this initial investigation, either because of interactions of the shock-hardening with second-phase particles, the necessity to optimize heat treatments, the influence of particle shape [15] or the existing work-hardened structure of oxide dispersion hardened powders. Standard powders, it was believed, would allow more information on the properties due to the consolidation

*Registered Trade Mark of Allied Corp.

technique to be ascertained. The initial objectives of this work were to determine how dynamic compaction affected the fatigue properties of material, especially the effect of the particle bonding with its rapidly solidified weld zone and whether the highly work-hardened structure was beneficial or was lost by rapid work-softening. The attainment of the highest possible fatigue properties for aluminium alloys was not an objective at this stage.

2. Experimental details

Details of the dynamic compaction facility and compaction procedure have been previously presented [13–15]. For this work, compactions were produced using the experimental two-stage device and the single-stage compaction machine. The powder experienced similar conditions in each case and the compacts had similar properties. For the single-stage press these are easily attainable conditions and do not involve high pressures on the compaction chambers or dies.

Compaction was carried out under a medium vacuum. However, total exposure time to the vacuum was less than 15 min. No degassing at "high temperature" was employed, although this is usually considered essential for high-strength aluminium PM [2, 19].

2.1. Material

Commercially pure (99.7%) aluminium atomized powder from Ecka Gbm with an average particle size of 120 μm was used. Subsequently, this was changed to a similar powder with an average particle size of 70 μm.

2.2. Testing

Standard fatigue, tensile and hardness tests were carried out on the as-compacted material. The fatigue tests were to determine the SN curve under alternate tension/compression loading. These tests were carried out by EMPA, the Swiss Federal Laboratory for Testing Materials and Research. A vibraphone testing machine was used at a frequency of 90 or 100 Hz. Small rectangular fatigue specimens were employed, and this permitted about six specimens to be obtained from every compact. It was thus possible to determine if compactions carried out under conditions believed to be identical had similar fatigue properties.

Specimens from the same compact had reasonably identical shapes. However, some variation in size existed between specimens taken from different compacts. The initial specimens had a section of around 4 mm x 6 mm or 4 mm x 8 mm. These, however, had a tendency to break at the grips, necessitating a reduction in the section to around 4 mm x 4.5 mm. The specimens were machined by standard techniques. The final machining was carried out by EMPA, the specimens were left in the as-milled conditions. Surface finish was therefore good, but could have been improved.

In general, the test specimens were shorter than those normally employed for the test machine and this resulted, in some cases, in a slight bending force on the specimens. This problem was largely overcome by EMPA in the first tests, but may have resulted in some erratic results in two series of specimens which were brittle and had a low strength. The measures taken by EMPA are believed to have ensured that this did not affect the results reported, although ideally, tests with larger specimens would have been preferred.

3. Results and Discussion

3.1. Preliminary tests

Trial experiments were carried out to determine the order of magnitude effect on fatigue life of dynamic compaction. A billet of aluminium compacted from powder with a mean particle size of 120 μm on the two-stage machine was cut up to give eight rectangular strips, which were then milled to the test piece shape. These specimens were tested in the as-compacted condition. Unfortunately, they were smaller than normal specimens and therefore tended to break in the grips. This was avoided by re-machining to obtain a smaller area for the test section.

In view of the few specimens available, the fatigue limit was initially estimated by retesting unbroken specimens at higher loads (comparison with subsequent results indicated that this did not substantially alter the fatigue limit). The results of the first tests are shown in Fig. 2. Results from specimens which did not break down at the minimum section are also shown as they give a minimum value. From Fig. 2 a fatigue limit of over 62 MN mm^{-2} at 10^7 cycles can be estimated, which is a much higher value than the 30 to 40 MN mm^{-2} at 10^7 cycles of the wrought ingot metallurgy material of similar composition, Table I. The tensile strength of the compact was around 200 MN m^{-2}. This gives a fatigue ratio of around 0.31. From the mechanical proper-

TABLE I Mechanical properties of ingot metallurgy wrought aluminium; the fatigue data is for 2 to 4 mm thick rectangular test pieces with non-machined surfaces. From Technical Data for Wrought Products of Al alloys – Swiss Aluminium, Zürich.

DIN and Alusuisse designations	Tensile strength ($N\,mm^{-2}$)	0.2% proof stress ($N\,mm^{-2}$)	% elongation	Brinell hardness	Alternating strength fatigue strength at 10^7 cycles ($N\,mm^{-2}$)	Ratio
Al 99.5%						
Annealed	65 → 95	20 → 55	40	20	30	0.31 → 0.46
1/2 Hard	110 → 150	90 → 145	9	35	30	0.20 → 0.27
Hard	≧ 150	≧ 130	3	45	40	≦ 0.26
Al Mn "Aluman 100"						
Annealed	90 → 130	35 → 80	28	28	40	0.31 → 0.44
1/2 Hard	140 → 180	110 → 170	10	45	40	0.22 → 0.29
Hard	≧ 185	≧ 165	3	60	50	≦ 0.27

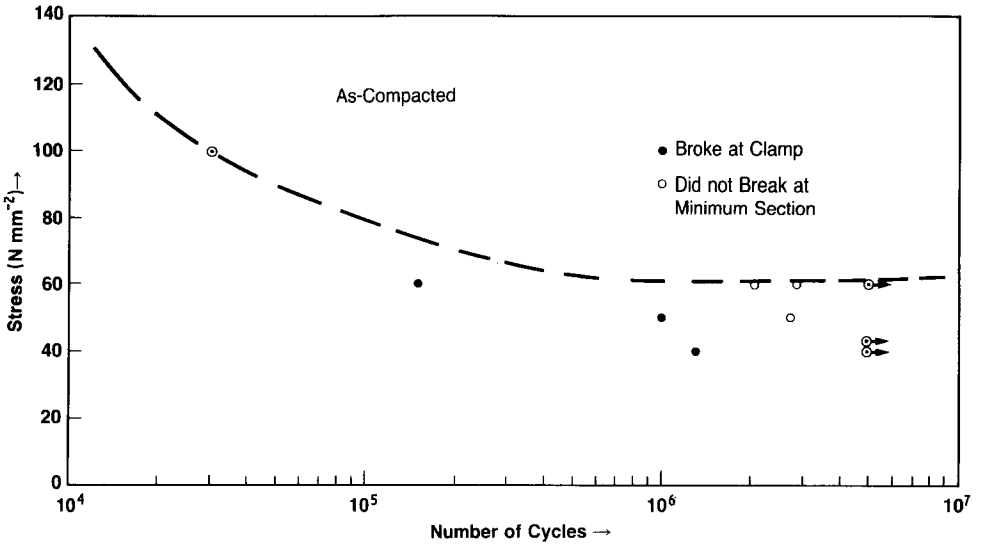

Figure 2 Initial trial tests, showing the fatigue life as a function of stress. Specimens taken from one billet of dynamically consolidated aluminium.

ties in Table I, a fatigue ratio can be calculated for the ingot metallurgy material. This decreases as the work-hardening increases (Table I). For the "fully" hardened condition a value of 0.27, or lower, is obtained for the two materials considered. The ingot metallurgy alloys have, therefore, a fatigue ratio which appears to be less than that of the dynamic compact. As the dynamic compact has undergone more work-hardening (it has a higher hardness), it would be expected to have a lower fatigue ratio than the ingot metallurgy material. It was thought, therefore, that the improved fatigue limit of the dynamic compacts was due to a superior tensile strength and to a slightly higher fatigue ratio. These results were considered to justify a more detailed investigation.

3.2. Effect of compaction parameters

To try to determine the important parameters specimens were produced with different mechanical properties. The specimens were fabricated mostly on the single-stage press, but a few were made on the double-stage launcher. The conditions of compaction were chosen so as to produce significant interparticle melting and bonding as defined by the value of the ratio R in Equation 1 [21]. Values of R above 1 produce good bonding.

$$R = S[d(1-a)(a^{5/2}b^{5/2}T_sC_pK\rho^{3/2})^{-1}] \times (bP)^2(1+bP)^{1/2} \quad (1)$$

where d is the effective mean size of the powder particles, C_p is the specific heat of the solid material, K is the thermal conductivity of the solid material, T_s is the melting point of the solid material, ρ is the density of the solid material, P is the compacting pressure behind the shock wave, b is the compaction constant representing the powder's stiffness defined by the pressure density relationship [22], a is the initial density of the compact [22], and S is a shape factor describing the geometry and initial state of the particles' surface. Values of S have been determined for different types of powders [21, 23]. The theoretical basis for Equation 1 has been presented previously [24]. Its validity has been shown for metal and some ceramic powders [14, 21, 23, 24]. The use of Equation 1 allowed identical compaction conditions to be attained on each facility. The specimens were tested as compacted and after annealing at 300 and 400° C.

Specimens were also produced at a value of R below 1, where good bonding does not occur. However, they have been shown to undergo appreciable activation of sintering [24, 25]. Appreciable strengths and toughness values are obtained by sintering at temperatures as low as 300° C [24, 25]. These specimens were tested after annealing/sintering at 300, 350, 450, 550 and 600° C.

For comparison with the fatigue properties, the standard tensile properties were obtained for all the different compaction and annealing conditions. These were obtained using a conventional Instron testing machine. Static tensile data were also

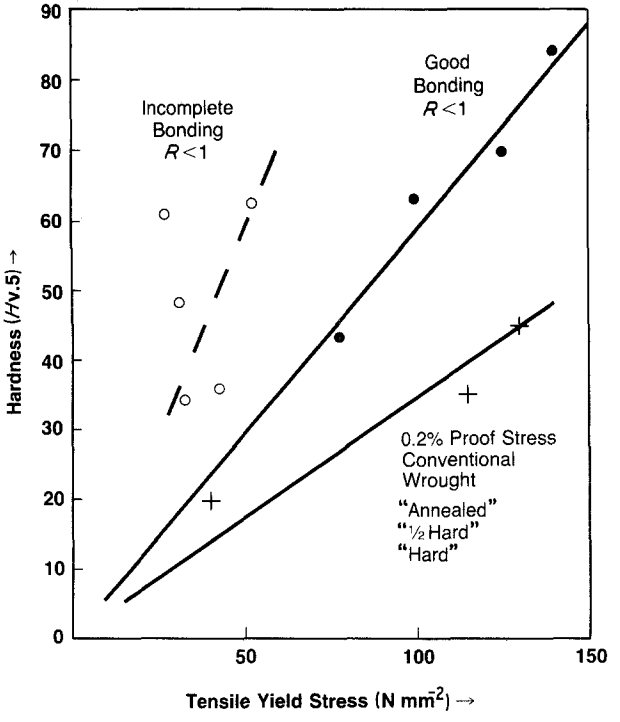

Figure 3 Effect of annealing at temperatures of 300 to 450° C on the range of mechanical properties of aluminium compacts produced at "medium" and "high" velocities.

obtained by EMPA on some of the high velocity compacts. The EMPA data confirmed that obtained on the Instron.

The yield stress hardness plot in Fig. 3 shows the wide range of property combinations that were tested. These properties are compared to those of a similar wrought alloy in the annealed, 1/2 Hard and Hard condition. For the conventional material the somewhat higher 0.2% PS is used. The well-bonded compact can be seen, for a given yield stress, to have around twice the hardness of wrought material, even when annealed. It has previously been reported for dynamically compacted stainless steel that some shock-hardening is retained after annealing [14].

It is to be noted that the as-compacted dynamically compacted material has not only a higher hardness and tensile strength than the wrought material in the "Hard" condition, but also a slightly higher ductility, around 6% compared to 3%.

For the well-bonded material ($R > 1$) and the conventional wrought material a definite relationship exists between yield stress and hardness. It is not clear that such a relationship exists for the incompletely bonded ($R < 1$) compacts.

The fatigue strength of well-bonded compacts ($R > 1$) (Fig. 4), did not show any difference between specimens produced on the two facilities. The fatigue strength did, however, decrease slightly for specimens annealed at 300° C, where a small to negligible hardness decrease occurs, and decreased significantly for the specimens annealed at 400° C where appreciable softening occurs.

The specimens produced at conditions which result in incomplete bonding ($R < 1$) and which were then annealed showed a very low fatigue strength after annealing at 300° C. The fatigue strength of these specimens increased with the annealing/sintering temperature. This indicates that low-temperature activated sintering may produce acceptable strength and toughness properties [24, 25], but produces poor fatigue properties due presumably to the diffusion bonds being weaker than those produced during dynamic compaction. When the temperature is high enough to produce good bonds the material has been significantly annealed. This is shown in Fig. 5 where the effect of annealing on the fatigue limit of "high" and "medium" impact velocity compacts is given. It is to be expected that a higher impact velocity than the "medium" velocity used, for example with a value of $R = 1$, would produce a compact which would undergo a more significant activation of sintering and properties between those indicated in Fig. 5. The as-compacted tensile strength of this

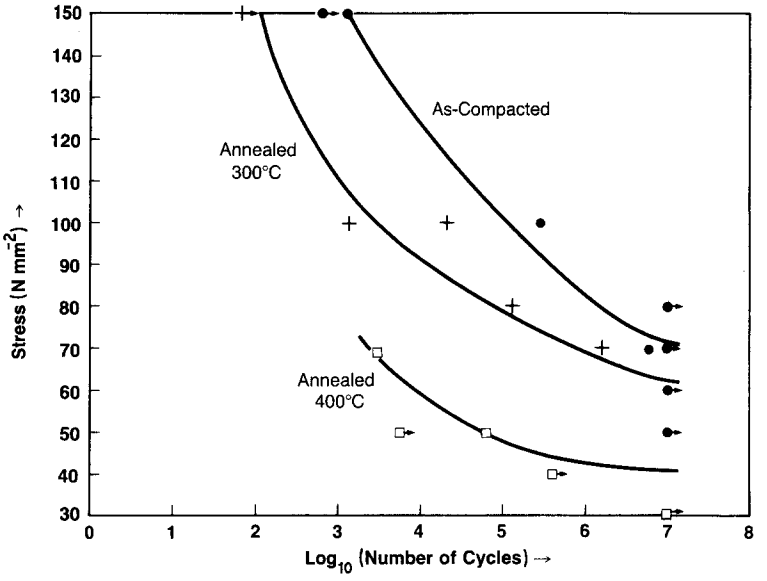

Figure 4 Fatigue life of well-bonded aluminium compacts tested as-compacted and after annealing for 1 h at 300 and 400° C. Specimens were produced primarily on a single-stage machine.

material would similarly be between the 30 and 248 N mm^{-2} reported, Table II, for the "medium" and "high" velocity compacts.

The tensile properties and fatigue strength at 10^7 cycles for all the compaction and annealing conditions are given in Table II. The fatigue ratio (fatigue strength at 10^7 cycles/UTS) is also given. It can be seen that the high-strength compacts do have a slightly higher ratio than high-strength conventional aluminium.

A plot of the fatigue strength at 10^7 cycles versus the ultimate tensile strength (Fig. 6), shows one straight line relationship that does not go through the origin for the well-bonded material ($R > 1$), while another apparently exists for incompletely bonded compacts ($R < 1$) and conventional wrought aluminium. From these plots the fatigue ratio appears a poor approximation. However, the use of the yield stress (Fig. 7), allows all the data for the compacts to lie on one straight line which passes through the origin. A fatigue ratio based upon the yield stress appears, there-

TABLE II Tensile properties and fatigue strength for different dynamic compaction and post-compaction annealing conditions

Velocity	Ratio R	Anneal	Yield stress (N mm^{-2})	UTS (N mm^{-2})	% elongation	$H_V \cdot 5$	Fatigue strength at 10^7 (N mm^{-2})	Ratio $\frac{\sigma\ 10^7}{\text{UTS}}$
"High"	$R > 1$							
		Initial specimen						
		as-compacted	100	202	4	63.0 (4)	62	0.31
		Subsequent specimens						
		as-compacted	140	248	8	83.0 (3)	70	0.28
		300° C	125	180	4	70.0 (8)	62	0.34
		400° C	77.5	106	6	43.0 (2)	40	0.38
"Medium"	$R < 1$							
		as-compacted		30		60 (8)		
		300° C	27.0	33.0	0.5	61.0 (4)	22.5	0.69
		350° C	52.5	103.0	0.9	62.5	27.5	0.27
		450° C	31.5	59.0	1.0	48.0 (6)	25.0	0.43
		550° C	32.5	121.5	28	34.5 (2)	30.0	0.25
		600° C	44.0	106.5	20	35.5 (2)	30.0	0.28

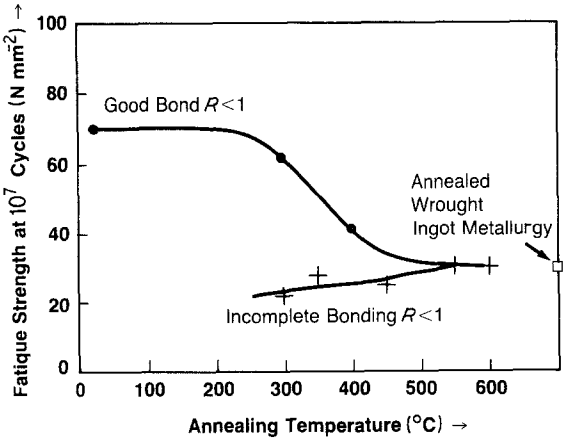

Figure 5 Effect of annealing on the fatigue limit of well-bonded and poorly bonded compacts.

fore, to be more valid for the dynamic compacts. The conventional wrought material also fits on the same plot in the annealed condition, but the 1/2 Hard and Hard material has a lower fatigue strength for a given yield strength, so indicating another type of relationship for wrought material.

Therefore, for the dynamic compacts the fatigue strength at 10^7 cycles is approximately given by

$$\text{fatigue strength at } 10^7 = 0.5 \text{ (yield stress)}.$$

3.3. Cyclic stress–strain curve

The high degree of work-hardening of the dynamic compacts raises the interesting question of what their response to low-cycle cyclic deformation would be. A high, even catastrophic, degree of work-softening can be imagined. The extremely high dislocation density could be in a very metastable state, so the work-softening usual with a work-hardened structure would be accelerated.

The well-bonded compacts, $R > 1$, were tested both in the as-compacted condition, and after annealing at 300° C; this anneal does not significantly reduce the compacts hardness. Static and cyclic stress–strain curves were run by EMPA. Final machining of the minimum section to a size of around 3 mm x 6 mm was again carried out by EMPA. This small size originally presented problems in strain determination, but this was resolved by fixing a Hottinger type LYG.3/120 strain gauge to the flat side of the minimum section, its active length being 3 mm.

The tests were run in a Schenck 40 kN servo hydraulic testing machine. The static tests were performed under load control with a stress gradient of 48.5 N mm^{-2} min^{-1}.

The cyclic stress–strain curve was determined by using an incremental step test, which subjects the specimen to blocks of gradually increasing and then decreasing strain amplitudes [26]. The strain gradients used were (1 to 4) x 10^{-4} sec^{-1}. The block comprised cycles which increased and then decreased in 1/10 increments of the total strain. The range of total strain investigated was (1 to 4) x 10^{-3}.

Tests were run with an increasing number of

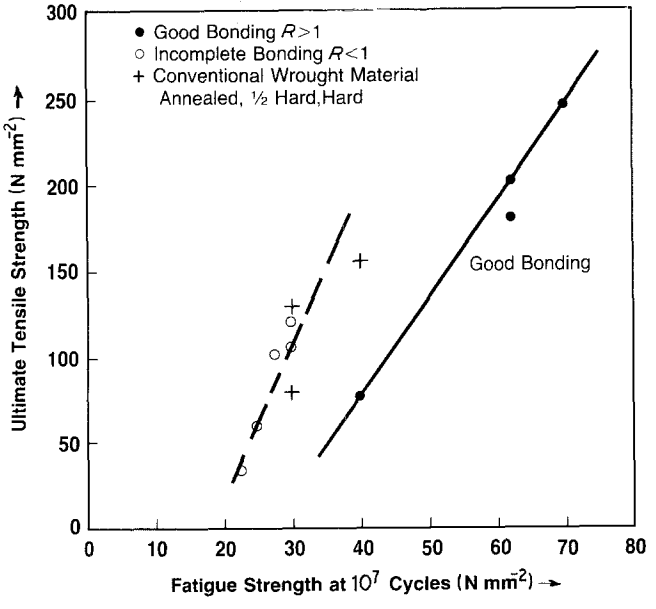

Figure 6 The relationship between the fatigue limit and ultimate tensile strength of aluminium compacts produced at medium and high velocities; the properties are for as-compacted and annealed material.

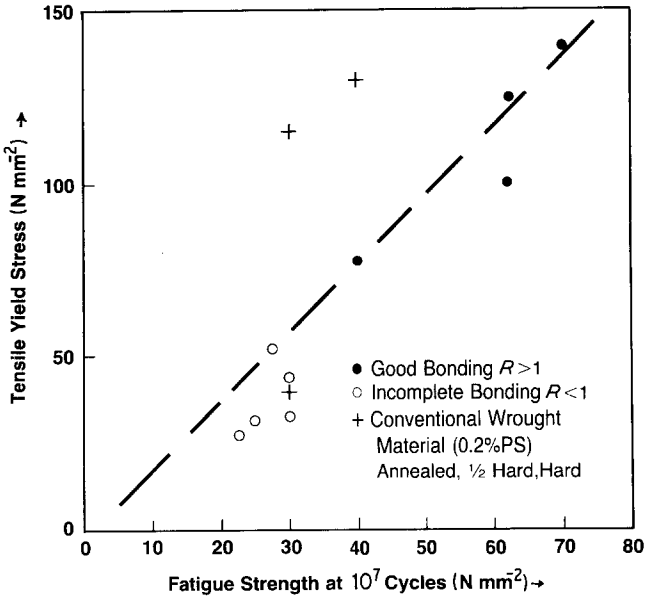

Figure 7 The relationship between the fatigue limit and tensile yield strength of aluminium compacts produced at medium and high velocities, tested as-compacted and annealed.

identical blocks (Fig. 8) to determine if, and when, a stable cyclic stress–strain curve was obtained. It was found (Fig. 9) that the as-compacted specimens exhibited a constant unique stress–strain curve from five blocks onwards, while the specimens annealed at 300° C exhibited a small but constant decrease in stress for a given strain up to the maximum number of blocks run for these specimens, 10. However, for both sets of specimens the change in the cyclic stress–strain curve after 1 block is small and even the 300° C annealed specimens may be considered as close to a constant stress–strain curve after 5 blocks.

Contrary to expectations, the as-compacted material underwent very little cyclic softening (Fig. 10), indicating that the as-compacted work-hardened structure was extremely stable. However, the small difference between the static/monotonic

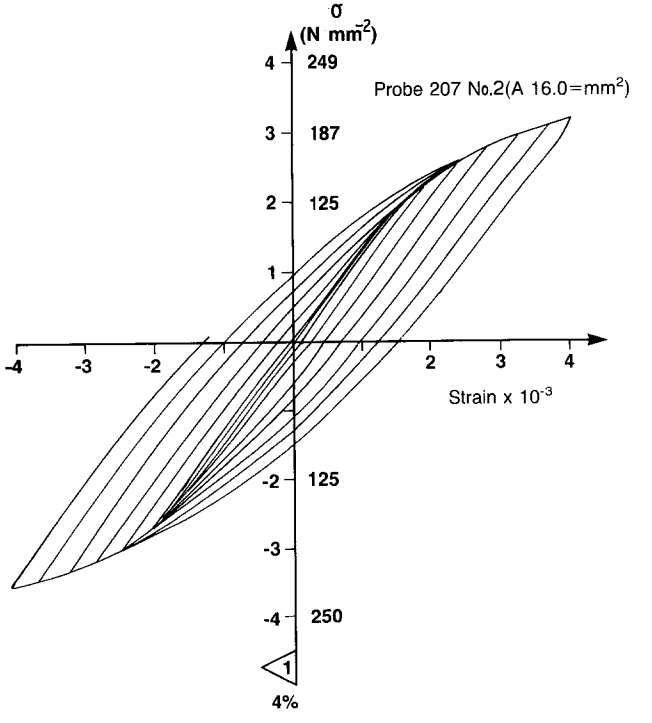

Figure 8 The stress–strain record for the first "block" of the incremental test to determine the cyclic stress–strain curve of the dynamically compacted aluminium.

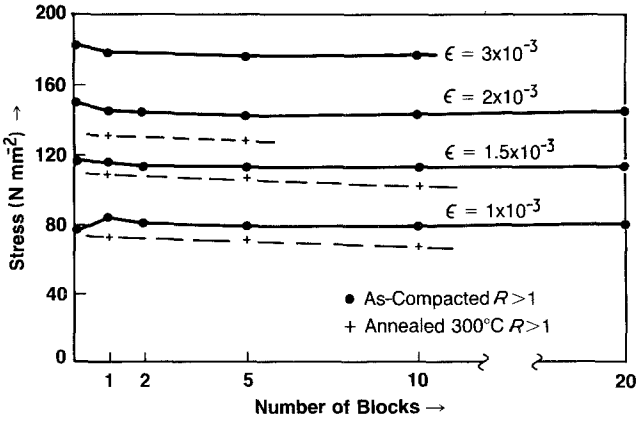

Figure 9 Cyclic hardening/softening as a function of the number of cycles (blocks) of the strain amplitude. For well-bonded material tested as-compacted and after annealing at 300° C.

and cyclic stress strain curve shown in Fig. 10 is a real difference; both the static and cyclic curves were confirmed on separate specimens.

The specimens annealed at 300° C underwent significant cyclic softening (Fig. 11). Presumably, the low-temperature anneal allowed the dislocations to undergo some rearrangement, and the new structure was more susceptible to cyclic softening than the as-compacted structure. However, the static stress–strain curve indicates a higher stiffness than the as-compacted specimens and was obtained from only one test. Its accuracy has not, therefore, been confirmed. Even if this static curve is inaccurate, the cyclic curve, which was confirmed on several specimens, does continue to decrease with the number of blocks run (Fig. 9), and is lower than the cyclic curve of the as-compacted material, indicating that the 300° C annealed specimens do undergo more cyclic softening than the as-compacted specimens.

It appears, therefore, that the work-hardened structure of as-compacted material is resistant to cyclic softening as it has been previously found to be resistant to thermal annealing [14]. However,

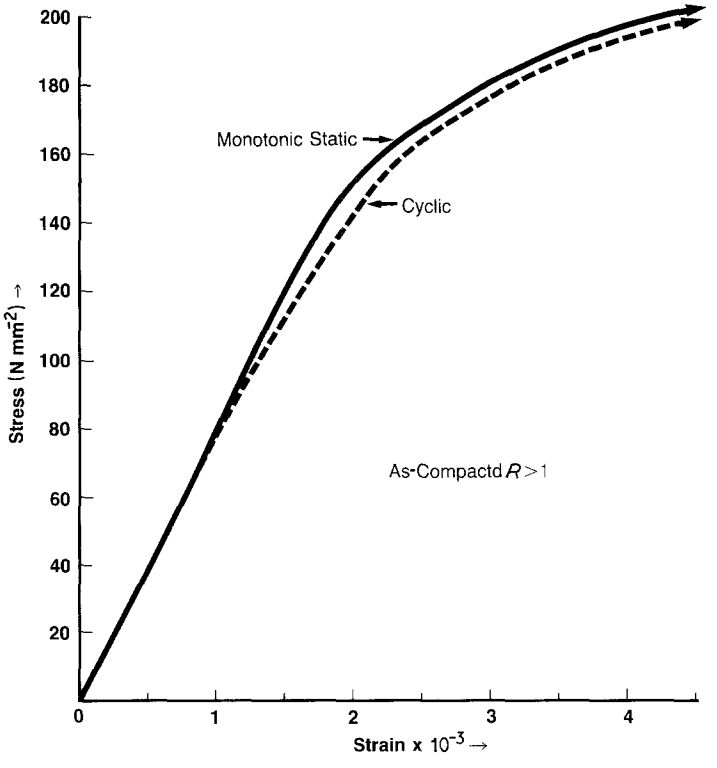

Figure 10 Monotonic and cyclic stress–strain curve for well-bonded aluminium tested as-compacted.

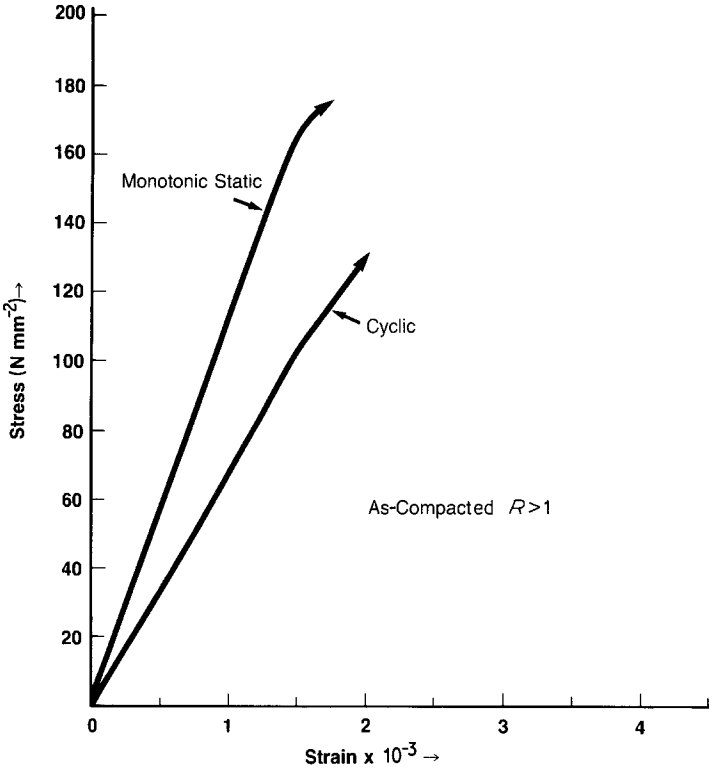

Figure 11 Monotonic and cyclic stress–strain curve for well-bonded aluminium tested after annealing at 300° C.

once it is thermally annealed, even if no appreciable difference in hardness is detected, the material does become more susceptible to cyclic softening.

Transmission electron microscopy (Fig. 12), shows that the as-compacted material has very fine sub-grains which contain dislocations within them; after annealing at 300° C the sub-grain size is unchanged (Table III) but the dislocations disappear from within the sub-grains. After the 400° C anneal high-angle boundaries are formed on which some precipitate appears, despite the aluminium being nominally unalloyed. Some low-angle boundaries, however, can still be detected and the sub-grain/grain size, while increasing, is still fine (Table III). It can be expected that a similar modification, as shown in Fig. 12, occurs in the rapidly quenched interparticle welds.

It would appear, therefore, that the greater resistance to cyclic softening of the as-compacted material compared to the material annealed at 300° C is due, at least in part, to the existence of a higher dislocation density within the sub-grains.

3.4. Fractographs

The fracture surfaces of specimens with different fatigue lives and different thermal treatments were examined by scanning electron microscopy. A Cambridge microscope was used at the Federal Polytechnic of Lausanne.

The investigation was not as detailed as desired; however, clear differences were found between the fracture surfaces of as-compacted and annealed specimens. In all the specimens, little evidence of fatigue failure, i.e. striations, was found, perhaps because of the nature of the tension compression test, and the powder metallurgy nature of the material. Striations when they were found appeared to be associated with the specimens' surface, but were not necessarily at the surface.

A comparison (Fig. 13) was made with tensile

TABLE III The sub-grain size after dynamic compaction and after annealing at 300 and 400° C. Note that after the 400° C anneal high-angle boundaries are also present

	As-compacted	Annealed	
		300° C	400° C
Average sub-grain size (μm)	0.80 ± 0.3	0.80 ± 0.3	1.10 ± 0.35

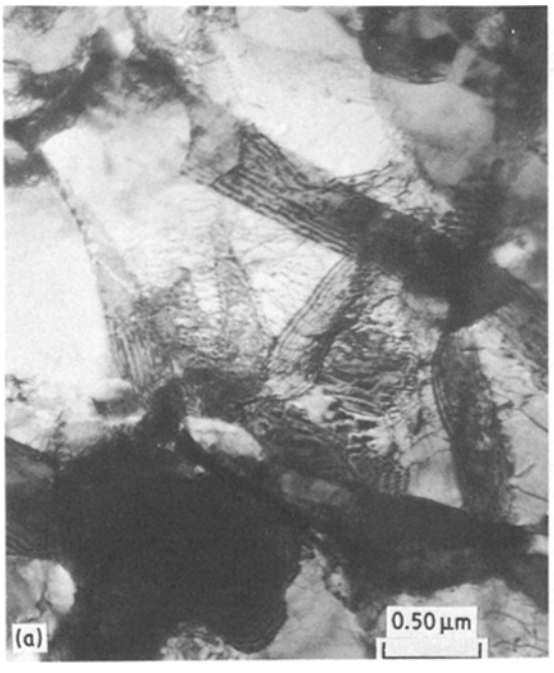

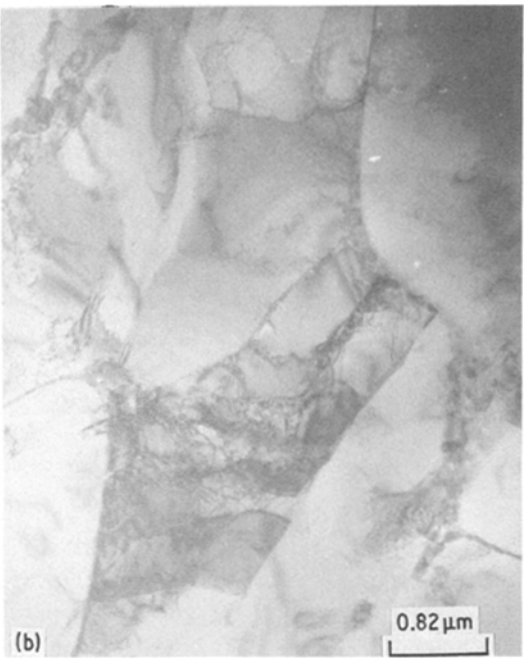

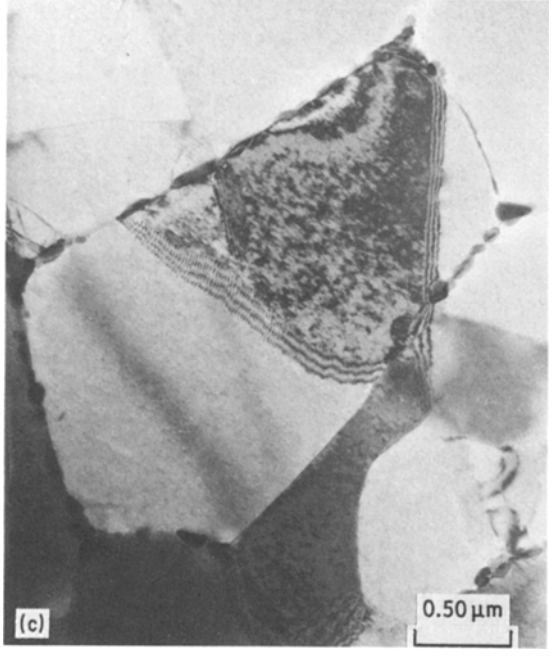

Figure 12 Typical transmission electron micrographs showing the structure within the particles in (a) the as-compacted condition, and after annealing for 1 h at (b) 300° C and (c) 400° C.

specimens of as-compacted material, $R > 1$. Failure can be seen to be ductile, as would be expected from the reported elongation. The ductile regions appear, however, to be non-uniform and may be situated around the circumference of particles, perhaps associated with melted material.

The as-compacted material, $R > 1$, exhibited a less ductile interparticle failure in fatigue. This was often characterized by "ridges" or "cliffs" as in Fig. 14. These appeared especially visible near the origin of the fracture and may be connected with points at which the crack opening was temporarily stopped. However, examination of the machined surface close to the fracture indicates that several potential fracture origins were also opening up prior to failure, so the "ridges"/"cliffs" may be origins of failure.

In the regions away from the origin the fracture surface was often associated with small round particles, as in Fig. 15. These might be oxide or metal from the surface of the powders already accumulated by the shock wave during compaction, impurities in the 99.7% pure aluminium, or associated with the rapidly solidified weld zone. An analysis of those inclusions has not as yet been conducted.

However, recent work [27] has shown that similar shapes are formed from fatigue wear debris in a PM aluminium alloy, but not in a wrought alloy. The spheres are thin platelets of aluminium produced by the rubbing together of the surfaces of a crack. These platelets eventually roll up

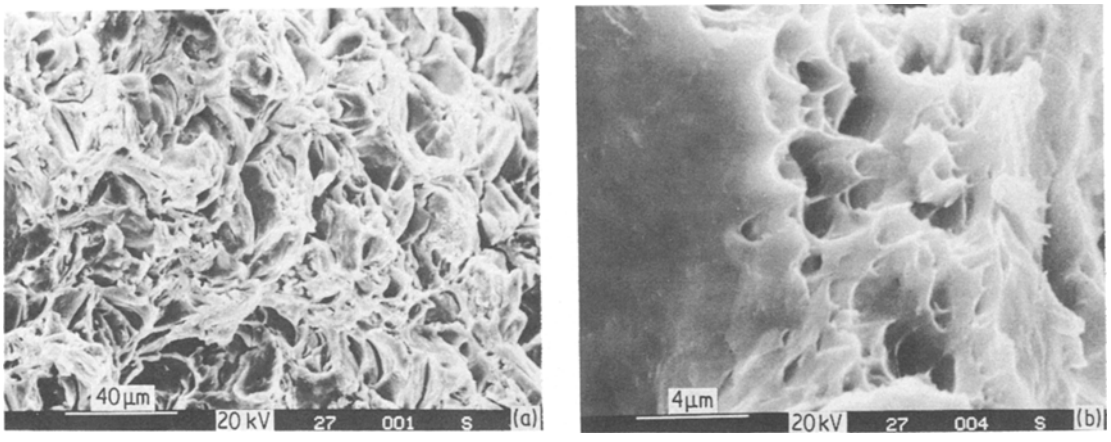

Figure 13 Scanning electron micrographs showing the ductile fracture associated with the as-compacted tensile specimens.

into spheres [27]. However, such spheres have only been reported for tests in vacuum. The spheres were not observed for tests in air, and it was assumed that this was due to oxidation of the platelets. The present work was, of course, in air. A further difference is that the present spheres are somewhat larger than those reported [27]. Further work to determine if the present spheres are definitely wear debris could give us additional information about the type of fatigue failure and perhaps about the compaction mechanism.

The specimens annealed at 300° C show a greater ductility (Fig. 16), and the spherical particles are still present.

After annealing at 400° C the fracture shows greater ductility, but is still interparticular (Fig. 17). The spheres may be detected, but are not as apparent as for the 300° C annealed material.

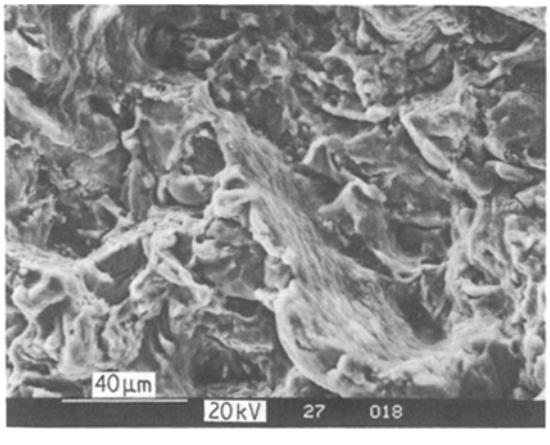

Figure 14 Scanning electron micrograph showing a "ridge" observed with the as-compacted fatigue specimens.

The specimens produced at a lower impact velocity, $R < 1$, and then annealed at 300° C, had a fracture surface which showed no sign of ductile failure and which allowed easy identification of the original powder particles (Fig. 18). If the fracture of the high-impact velocity material could be imagined as from a cast or wrought material, the fracture of the lower impact velocity material, even after annealing at 300° C, is indicative of a poorly sintered powder metal product.

3.5. Origin of the fracture

All the specimens examined were studied to try and determine the point of commencement of fracture. This met with varying success; with the 400° C annealed specimens it was possible to make a definite determination of the origin. However, for the as-compacted specimens definite determination was not possible, although identification of its probable origin was possible.

In Fig. 19 the origin of a high-velocity, $R > 1$, specimen that has been annealed at 400° C is shown. The relatively small area covered by fine striations is typical. Larger striations interconnecting several particles which are not neighbours may also be seen. A substantial amount of fretting deposit on the fracture surfaces indicates that complete failure occurred some time after the crack opened up.

For the as-compacted material, $R > 1$, evidence of fine striations was not found, but broader grooves were found (Fig. 20), in the "ridges" which could be associated with the origin of failure. The suspected area of origin often contained an appreciable amount of fretting deposit and several areas made up of the grooves.

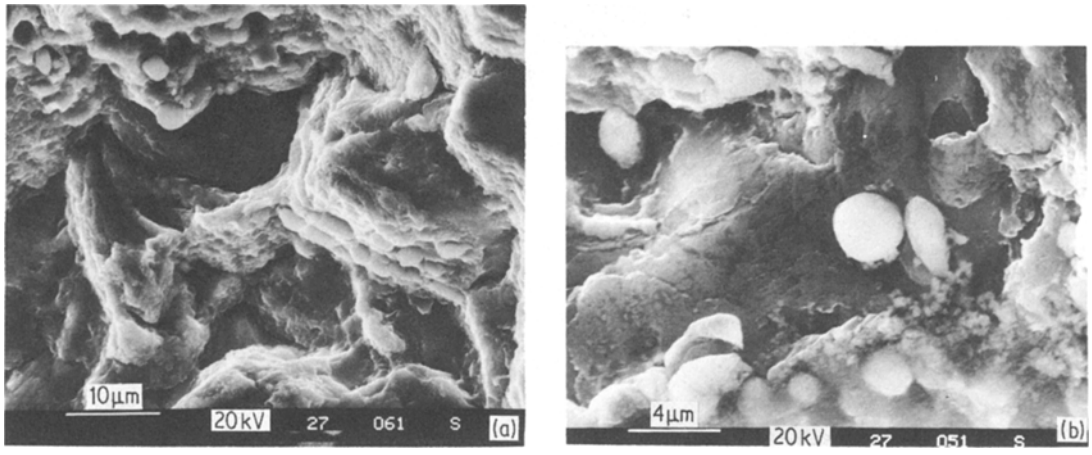

Figure 15 Scanning electron micrographs showing the "inclusions" associated with the as-compacted fatigue specimens.

Failure was interparticular; it was not, however, determined if failure was due to the interparticle bonds or commenced at areas of oxide or areas at which interparticle bonding did not occur. Recent work on wrought PM attributed the commencement of failure to oxide particles [28]. Further work is required in this area to determine, for instance, if degassing would further improve the properties.

4. Conclusions

The unique structure, of shock-hardened particles, bonded together by rapidly solidified welds, produced by dynamic compaction, results in aluminium compacts with significantly higher fatigue strengths than wrought ingot metallurgy material of similar composition. In addition it has been been found that:

1. the fatigue strength is highest for well bonded material, $R > 1$. Probably, the fatigue strength increases with R;

2. interparticle bonding and a high hardness are both important. Annealing well-bonded material, $R > 1$, decreases the hardness and hence the fatigue strength. However, for the poorly bonded material, $R < 1$, annealing increases the bond strength and hence the fatigue strength;

3. the fatigue strength of the dynamic compact appears to be more directly related to the yield strength rather than the ultimate tensile strength as for wrought material. It is proposed for dynamic compacts a relationship of the type: fatigue strength at $10^7 = 0.5$ (yield strength);

4. the as-compacted dynamic compacts have a stable dislocation structure and undergo a small but still reproducible amount of cyclic softening.

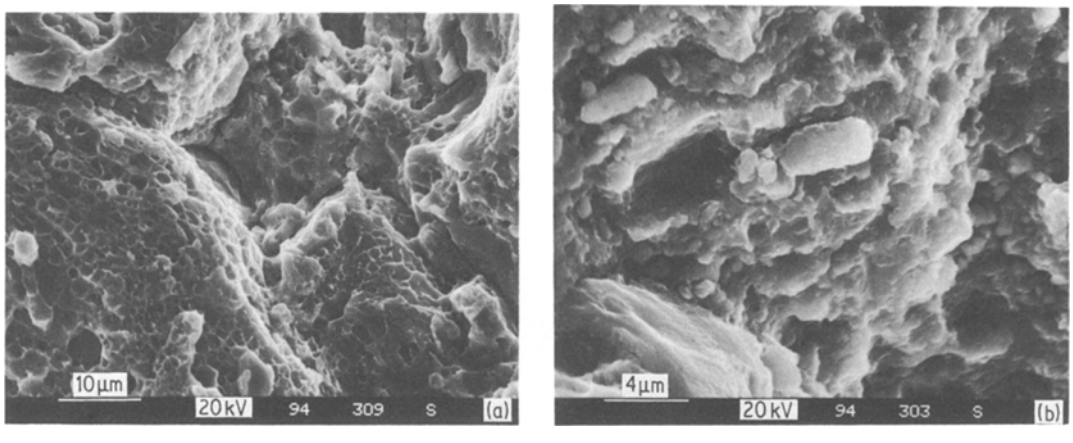

Figure 16 Scanning electron micrographs showing "inclusions" and evidence of ductile failure observed in specimens annealed at 300° C prior to fatigue testing.

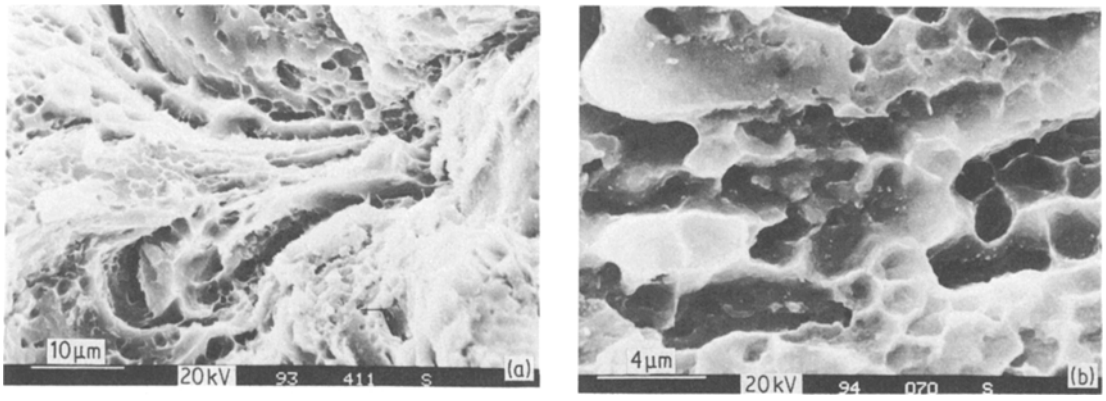

Figure 17 Scanning electron micrographs showing the more ductile failure of specimens annealed at 400° C prior to fatigue testing.

However, thermal annealing at 300° C resulted in the material undergoing a more significant amount of cyclic softening. This appears to be at least partly caused by the anneal reducing the number of dislocations within the sub-grains;

5. fracture micrographs show that the material fails in a ductile interparticle manner, and that the ductility increases with annealing temperature. The fatigue specimens show "ridges" and inclusions that warrant further investigation;

6. the good as-compacted properties combined with the observation that annealing and sintering decreases strength and increases ductility is an indication that surface oxide is sheared off during dynamic compaction and is not a major problem, suggesting that high-temperature degassing is not essential for dynamic compaction.

The improved fatigue properties for aluminium are believed to be characteristic of the technique, but obviously this must be confirmed by further work on other materials.

Acknowledgements

The compacts were produced at Inst. Cerac, Lausanne, Switzerland by the author. The assistance given by Dr G. Cooper and F. Capuano is especially appreciated. The fatigue tests were conducted by Dr V. Esslinger of EMPA, Zurich, 8600, Switzerland. His co-operation and the skill and accuracy of his department are gratefully acknowledged. The assistance given to the author by all of the Interdepartmental Department of Microscopy of the EPFL, Lausanne, Switzerland is also gratefully acknowledged, as is the work of Dr S. Das of

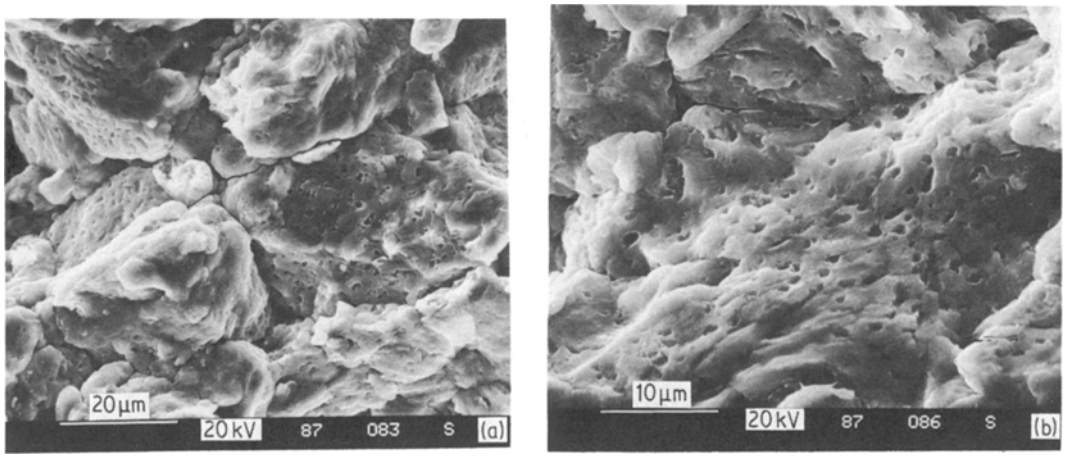

Figure 18 Scanning electron micrographs of the fracture surface of a fatigue specimen from a compact produced at a low impact velocity $R < 1$ and annealed at 300° C.

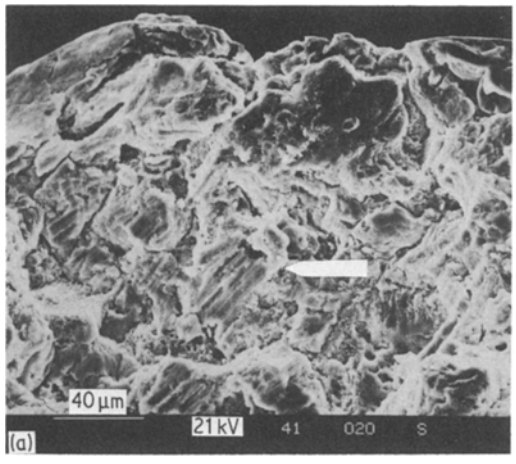

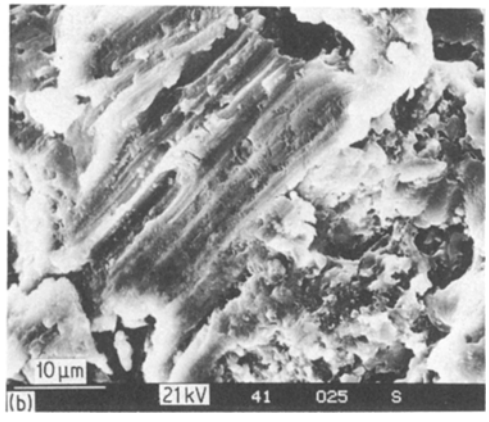

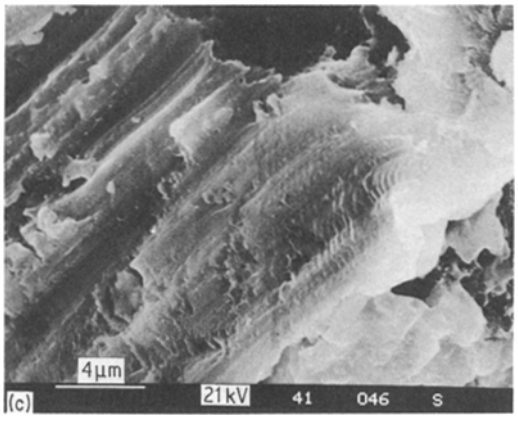

Figure 19 Scanning electron micrographs of the fatigue striations at the origin of failure for a fatigue specimen annealed at 400° C prior to testing. The point of origin is indicated in (a).

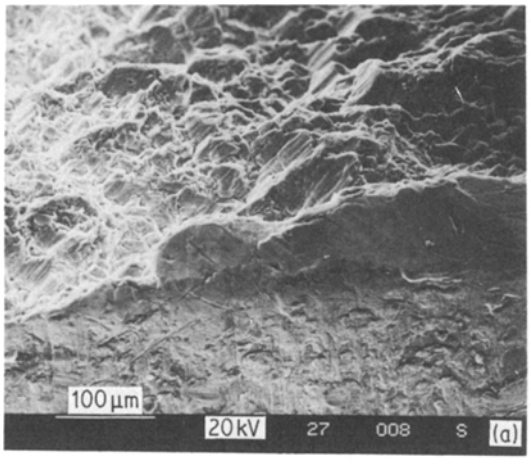

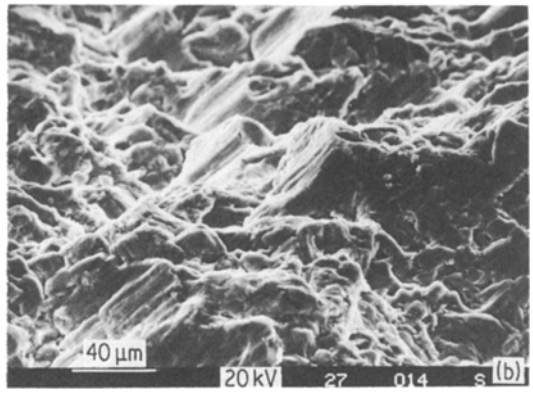

Figure 20 Scanning electron micrographs of the probable origin of failure of an as-compacted fatigue specimen.

Allied Corporation in producing the TEM micrographs of Fig. 12.

References

1. J. P. LYLE and W. S. CEBULAK, *Met. Eng. Q.* February (1974) 52.
2. W. S. CEBULAK, E. W. JOHNSON and H. MARKUS, *Int. J. Powder Met. Tech.* **12** (1976) 299.
3. H. W. ANTES, A. LAWLEY and M. J. KOCZAK, Proceedings US National PM Conference, Cincinnati (American Powder Metal Institute, Princeton, NJ, 1979).
4. G. T. BROWN and J. A. STEED, *Powder Met.* **17** (33) (1974) 157.
5. D. J. EVANS, D. N. DUHL and R. B. SLACK, "Modern Developments in PM", Vol. 8 (Plenum Press, New York, 1974) p. 473.
6. Y. G. KIM and H. F. MERRICK, 4th International Superalloys Conference, edited by J. K. Tien, S. T. Wlodek, H. Morrow, M. Gall and G. Maurer (American Society for Metals, Metals Park, Ohio, 1980) p. 541.
7. F. A. THOMPSON, C. P. CUTLER and R. J. SIDDALL, 108th AIME Annual Meeting, New Orleans (1979) and Henry Wiggan Technical Report 3184.
8. M. RAFLIN, M. J. KOCZAK and A. LAWLEY, Proceedings "Thermomechanical Processing of Aluminium", St. Louis (AIME, New York, 1979) p. 147.
9. M. T. JAHN, T. LIN and C. M. WAN, *J. Mater. Sci.* **15** (1980) 1870.
10. R. E. SANDERS, W. L. OTTO and R. J. BUCCI, AFML – Report – T.L. 79.4131, September (1979) American Airforce, Washington.
11. T. SHEPPARD, "Proceedings 2nd International Aluminium Extrusion Seminar", Vol. 1, (Aluminium Association, Washington, D.C., 1977) p. 331.
12. D. MACLEAN, "Mechanical Properties of Metals" (Wiley, New York, 1962).
13. D. RAYBOULD, "High Strain Rate Phenomena", edited by M. A. Meyers and L. E. Murr (Plenum Press, New York, 1981) p. 895.
14. *Idem, J. Mater. Sci.* **16** (1981) 589.
15. *Idem*, Proceedings "7th International HERF Conference", edited by T. Blazynski (University of Leeds, Yorkshire, 1981).
16. M. A. MEYERS and L. E. MURR, "High Strain Rate Phenomena", edited by M. A. Meyers and L. E. Murr (Plenum Press, New York, 1981) p. 487.
17. L. A. DAVIS, *J. Mater. Sci.* **11** (1976) 711.
18. Y. G. DOROFEEV, *Sci. Sintering* **12** (1981) 181.
19. J. R. PICKENS, *J. Mater. Sci.* **16** (1981) 1437.
20. M. E. FINE, *Met. Trans. A.* **6A** (1975) 625.
21. Swiss Patent 8204 77, Priority date 4 July (1977).
22. D. RAYBOULD, Proceedings of the "15th" International MTDR" Conference, Editors Tobias and Koenigsberger (Macmillan, London, 1975).
23. *Idem*, CERAC Report 502:1 (1976).
24. *Idem, Int. J. Powder Met. Tech.* **16** (1980) 2.
25. *Idem*, National PM Conference, Montreal, Vol. 38, edited by J. Bewley and S. McGee (APMI, New Jersey, 1982) p. 575.
26. R. W. LANDGRAF, J. MORROW and T. ENDO, *J. Materials* **4** (1969) 176.
27. J. LANKFORD and D. L. DAVIDSON, *Met. Trans. A* **14A** (1983) 1227.
28. S. HIROSE and M. E. FINE, *ibid.* **14A** (1983) 1189.

Received 2 September 1983
and accepted 13 January 1984